UCRL 3906
cy 2

UNIVERSITY OF CALIFORNIA

Ernest O. Lawrence Radiation Laboratory

BERKELEY, CALIFORNIA

DISCLAIMER

This document was prepared as an account of work sponsored by the United States Government. While this document is believed to contain correct information, neither the United States Government nor any agency thereof, nor the Regents of the University of California, nor any of their employees, makes any warranty, express or implied, or assumes any legal responsibility for the accuracy, completeness, or usefulness of any information, apparatus, product, or process disclosed, or represents that its use would not infringe privately owned rights. Reference herein to any specific commercial product, process, or service by its trade name, trademark, manufacturer, or otherwise, does not necessarily constitute or imply its endorsement, recommendation, or favoring by the United States Government or any agency thereof, or the Regents of the University of California. The views and opinions of authors expressed herein do not necessarily state or reflect those of the United States Government or any agency thereof or the Regents of the University of California.

UCRL-3906

UNIVERSITY OF CALIFORNIA
Radiation Laboratory
Berkeley, California

Contract No. W-7405-eng-48

THE SCATTERING OF K^+ MESONS IN EMULSION

George Igo, D. Geoffrey Ravenhall, Jerome J. Tiemann
Warren W. Chupp, Gerson Goldhaber, Sulamith Goldhaber, Joseph Lannutti
and Roy M. Thaler

September 24, 1957

Printed for the U.S. Atomic Energy Commission

THE SCATTERING OF K^+ MESONS IN EMULSION

George Igo, D. Geoffrey Ravenhall, Jerome J. Tiemann

Stanford University
Stanford, California

Warren W. Chupp, Gerson Goldhaber, Sulamith Goldhaber, Joseph Lannutti

Radiation Laboratory and Department of Physics
University of California, Berkeley, California

Roy M. Thaler

Los Alamos Scientific Laboratory
Los Alamos, New Mexico

September 24, 1957

ABSTRACT

Some new experimental results are presented, in two energy ranges, T_K = 40 to 100 Mev and T_K = 150 ± 30 Mev. An optical-model analysis is made of these results, which avoids many of the approximations of previous workers. It is concluded that the K^+ - nucleus interaction is repulsive and that the K^+ - nucleon cross section inside the nucleus is compatible with the observed cross section for free protons.

THE SCATTERING OF K^+ MESONS IN EMULSION

George Igo, D. Geoffrey Ravenhall,* Jerome J. Tieman**
Stanford University
Stanford, California

Warren W. Chupp, Gerson Goldhaber, Sulamith Goldhaber, Joseph Lannutti†
Radiation Laboratory and Department of Physics
University of California, Berkeley, California

Roy M. Thaler††
Los Alamos Scientific Laboratory
Los Alamos, New Mexico

September 24, 1957

INTRODUCTION

A considerable amount of information is now available on the nuclear interaction of K^+ mesons in photographic emulsions.[1-7] A certain part of this, the elastic differential cross section and the inelastic total cross section, is susceptible of a relatively unambiguous interpretation in terms of the optical model of the nucleus, and such an analysis has been made by many authors.[1-8] The contribution of this paper is, from the experimental side, to present new data in a higher energy range ($T_K = 150 \pm 30$ Mev), as well as to give some additional results in the range already covered by previous workers ($T_K = 40$ to 100 Mev). The object of the theoretical part of the paper is to analyse both sets of data in terms of the optical model. The analysis improves on that of previous workers in a number of respects, and the results are in some ways considerably different. In fact, in contradiction to previous work we find it impossible to deduce the sign of the K^+-nucleus potential from the lower-energy interaction. The data at the higher energy, however, allow us to conclude that it is positive (i.e., repulsive), although it is considerably larger than has been suggested by earlier authors. It is then found that the effective K^+-nucleon cross section inside nuclei is, after allowing for the Pauli principle, approximately the same as the cross section of K^+ mesons with free protons.

An analysis of the inelastic interaction of K^+ mesons will be given by some of us (J.E.L., S.G., and G.G.) in a separate article.[9]

EXPERIMENTAL DETAILS

The experimental technique used to determine the elastic differential cross section consisted of following K-meson tracks and measuring all elastic K^+-nucleus scattering events with projected angle in the plane of the emulsion larger than 2°.

For this work a nuclear-emulsion stack was exposed to a beam of positive K mesons of momentum 480 ± 30 Mev/c. We thus obtained information on the elastic scattering from the energy 220 Mev down to a low energy cut-off. A low energy cut-off was necessary because at low energies single scatters cannot be easily distinguished from multiple Coulomb scattering. Although this effect becomes predominant only at an energy $T_K \approx$ 20 Mev, we have chosen a cut-off energy of 40 Mev because the correction for small-angle detection efficiency was still appreciable up to this energy. We have compiled the data in two energy intervals, viz., 40 to 100 Mev and 100 to 220 Mev.

The angular cut-off of 2° was chosen by comparing the observed scattering with point-charge Rutherford scattering. From this comparison it was found that the detection efficiency decreases considerably below 2°. A geometric correction was made to take into account the loss of events introduced due to the 2° cut-off in projected angle.

The data for the energy interval (T_K = 40 to 100 Mev) is based on 18.1 meters of K meson track followed. We analyzed the scattering events in the form $\left\langle \frac{d\sigma}{dq} \right\rangle$, where $q = 2k \sin \frac{\theta}{2}$ (the recoil wave number), for reasons which will be discussed later.

Because our observed path length per energy interval in the region 40 to 100 Mev varied considerably with energy, a path length normalization was made. We divided the energy region 40 to 100 Mev into six equal energy intervals and weighted each scattering event by the inverse of the path length followed in the interval in which the scatter was observed. In compiling the data, we thus obtained

$$\left\langle \frac{d\sigma}{dq} \right\rangle = \frac{1/6 \ \Sigma \frac{1}{L_j} \left(\frac{\Delta N}{\Delta q} \right)_i}{\Sigma N_i} , \qquad (1)$$

where L_j is the path length observed in the jth energy interval; Δn is the number of scatters having q between q and $q + \Delta q$; Δq is the momentum transer interval and N_i is the number per cm^3 of each element in the emulsion excluding hydrogen. The $\left\langle \frac{d\sigma}{dq} \right\rangle$ distribution was converted to $\left\langle \frac{d\sigma}{d\Omega} \right\rangle$ and corrections made for the angle and energy cut-offs. The data for the energy interval 100 to 220 Mev is based on 75.8 m of K meson track. Figure 1 gives the path-length distribution observed in 10-Mev intervals. As an approximation to this distribution the calculations were made at the three energies shown, and the cross section obtained at each energy was weighted by the path length observed in the energy interval it represents, i.e.,

$$\left\langle \frac{d\sigma}{d\Omega} \right\rangle = \Sigma f_j \left(\frac{d\sigma}{d\Omega} \right)_j \qquad (2),$$

where $f_j = L_j / \Sigma L_j$. The three values of the weighting factors f_j and the energy intervals are given on the graph. In view of the almost normal distribution about 150 Mev, this high-energy data will be referred to as having an energy of $T_K = 150 \pm 30$ Mev.

Throughout this work, an attempt was made to determine whether each scatter was elastic or inelastic. Elastic interactions refer to those cases when the K meson interacted with the nucleus as a whole, and energy and momentum were conserved. In colliding with a light nucleus in emulsion this could result in a considerable energy loss for the K meson but then there would be a visible recoil. The measurement technique used to determine energy losses could reliably detect energy changes equal or greater than 10%. $\Delta T/T \geq 10\%$ was thus chosen as a criterion for inelastic events. This classification is not rigorously correct because it is possible to excite low-lying nuclear levels. Thus a K meson could have lost several Mev in such an inelastic scattering process and the loss would not have been detected and, consequently, the scatter would have been classified as elastic. Furthermore, in the high-energy interval the resolution is such that it is

possible for the K meson to knock out or cause the evaporation of one or two nucleons and yet have an energy loss of less than 10%. Three such events were found which had an energy loss of less than 10% and yet emitted an evaporation-type proton. These were included among the inelastic events. To correct somewhat for the corresponding events giving neutron emission, these events were weighted by a factor of two. This was actually a small correction to the cross section ($\sim 1\%$) but it shows the existence of the effect. It is difficult to make a reliable estimate of the number of such events to be expected. However, because the Pauli exclusion principle inhibits low-energy-momentum transfers for scatterings off single nucleons, one would not expect a large fraction of scattering events with energy losses less than 10%. Thus we feel that our inelastic cross-section determination (excluding nuclear-level excitation) is not seriously affected by the 10% cut-off criterion.

The observed cross sections for inelastic scattering in emulsion (including charge exchange) for the two energy intervals were

$$T_K = 40 \text{ to } 100 \text{ Mev}, \qquad \sigma_{inel} = 205 \pm 23 \text{ mb}$$

$$T_K = 150 \pm 30 \text{ Mev}, \qquad \sigma_{inel} = 284 \pm 20 \text{ mb}$$

THEORY

The starting point of the analysis of the data is the optical model of the nucleus: the elastic scattering of the K^+ mesons from the nuclei in the emulsion is calculated on the assumption that each nucleus may be represented by a smooth potential with both real and imaginary parts. This kind of analysis is by now familiar in its nuclear physics applications, and it is not necessary to elaborate on the actual mechanics of the calculation beyond saying that it involves a partial-wave analysis of the Schrödinger equation which makes essentially no approximation.[10] The form of the experimental data and the extent to which the nuclear parameters can be determined are somewhat different from other situations. It will be seen, however, that the essential features of our results should not depend critically on the particular values chosen.

Initially it is necessary to specify the four parameters characterizing the complex nuclear potential

$$(V + iW) \left[e^{(r-r_0)/d} + 1 \right]^{-1} \tag{3}$$

for each element in the emulsion. It is clearly not possible to determine all of these parameters with the present experimental data, so that r_0 and d, which fix the radial shape, are taken over from the results of other experiments. The radius and surface thickness of a nuclear potential presumably depend on both the nuclear-mass distribution and also the range of the interaction potential between the scattered particle and the nucleons. Because the K^+-nucleon interaction, while unknown at present, is expected to have a considerably shorter range than, say, the nucleon-nucleon interaction, we have chosen to set it equal to zero, and to use for the shape of the K^+-nucleus potential just the nuclear mass distribution. In fact we have used, instead of the mass distribution, which is not well known at present, the charge distribution,[11] which is probably not much different from it. Thus we take the values

$$\begin{aligned} r_0 &= 1.07\, A^{1/3} \times 10^{-13} \text{ cm}, \\ d &= 0.57 \times 10^{-13} \text{ cm}. \end{aligned} \tag{4}$$

These same parameters have been used also for the charge distribution itself, in the calculation of the Coulomb interaction. The choice of the remaining two parameters, V and W, is simplified because the experiment also measures the inelastic scattering.[11] Hence for any value of V the value of W can be fixed. Because the actual experimental number to be fitted is an average over both the elements in the emulsion and the incident energy, T_K, the actual choice of W could be made in many ways. For simplicity we have made the following choice: we have assumed that V and W are independent of element and energy in each of the energy ranges (although not the same in both, of course). For the various values of V we have considered, W has then been chosen after many trials to give an averaged total inelastic cross section that agrees with the experimental value in that energy range. The averaging over elements in the emulsion has been simplified by classifying all light nuclei as nitrogen, so that the emulsion is assumed to consist of silver, bromine, and nitrogen in the ratios

$$\mathrm{Ag:Br:N::0.22:0.22:0.56.} \tag{5}$$

We shall comment on the above simplifications later. (Experimentally, the hydrogen events beyond 7° are recognizable as such and are not included.)

The qualitative features of the elastic differential cross section can be well understood by considering the Born approximation for the process. In fact this approximation has been used to analyze earlier experiments,[1,4,8] although it is by now realized that in this application it is quantitatively unreliable. The essential features are that in the forward direction the cross section is dominated by the Rutherford cross section, while at large angles the scattering comes almost entirely from the nuclear potential. Of main interest to us is the angular region where the two types of scattering are comparable, and where the constructive or destructive interference between the two will be observed. It is fortunate that it is well separated from the region where diffraction effects due to the finite size of the nuclear potential occur, because our decision as to the type of interference will thus not be strongly influenced by our previous choice of the finite size. In the lower-energy range (T_K = 40 to 100 Mev) we have taken advantage of a clue given to

us by the Born approximation, and both experimentally and theoretically we have used as the independent variable not the scattering angle θ but the recoil wave number q; where

$$q = 2k \sin \frac{1}{2} \theta; \quad k = \left[2Mc^2 T_k + T_k^2\right]^{1/2} / \hbar c; \qquad (6)$$

and Mc^2 is the rest mass energy of the K meson. It turns out that in our exact partial-wave analysis, as in the Born approximation, the differential cross section plotted against q is surprisingly independent of energy. The advantage of the q plot is therefore that the averaging in energy does not wash out the details of the angular distribution. In the higher-energy region ($T_K = 150 \pm 30$ Mev), this was not done because of fractional range in energy is rather less, and the energy dependence of the differential cross sections plotted against θ is not so pronounced: consequently the advantage of the q-plot is then outweighed by the greater difficulty in analyzing the experimental data.

The important region for deciding on the magnitude of V (as distinct from its sign) is at large angles, where the scattering comes entirely from V. It is here that the choice of nuclear size and shape is important. However, the inelastic scattering is also large, so to avoid any uncertainty due to difficulty in identifying the events that are elastic, it is better to consider the total cross section (elastic plus inelastic). In order to exclude the region containing Rutherford scattering (which involves a large differential cross section depending very little on V) we calculate the total cross section (elastic plus inelastic) for angles greater than a certain θ_0.

NUMERICAL RESULTS

As will be seen, our final results are not in quantitative agreement with those of earlier workers, while our general method is quite the same. We think that the difference is due to an accumulation of small differences rather than any one effect. To make this clear, we will describe briefly the various stages of the analysis, and comment on the intermediate results.

First, in contrast to earlier authors,[1-4, 8] we have used a realistic shape for the complex nuclear potential, and have made an exact partial-wave calculation of the scattering due to it. The shapes used by other authors seem to have been selected for analytical convenience rather than for physical reality, being either square (no surface thickness), gaussian, or even exponential. As we have argued earlier, the shape chosen may not influence too much the decision as to the sign of V, but it will affect conclusions drawn about its magnitude.

Just as important a defect in the earlier work is the neglect of the imaginary potential in computing the elastic differential cross section. The change that this produces is illustrated in Fig. 2, where we show for V = - 20 Mev, a typical value, the differential cross section for both W = 0 and W = - 4.1 Mev; the latter value leads to a total inelastic cross section in agreement with experiment. Of great importance in this particular case, where the structure in the interference region is to be investigated, is the fact that the inclusion of W smooths out the interference minimum into a flat plateau. We understand this as the effect of adding to the scattering amplitude due to V a part due to W which is out of phase with it, and which is smooth in this region. The decrease of the cross section at larger angles due to W is, we feel, the influence of W in subtracting from the incident flux of particles as they pass through the nucleus, so that there is less flux to deflect. It should be remarked that the curve for W = 0 of Fig. 2 has a very much shallower interference minimum than that obtained by other authors[1, 4, 8] using the Born approximation.

With the assumption that V and W are the same for all nuclei in the emulsion and at all energies in the range, the choice of W for any selected V is made by calculating the total inelastic cross section σ_{inel} for a number

of values of W at the median energy, and taking the average of Ag, Br, and N according to the ratios of Eq. (5). That value of W which at this energy gives the experimental value for σ_{inel} is then obtained by interpolation. Although the values of σ_{inel} at the other energies then differ slightly from the experimental value, the differences almost disappear in taking the energy average. It is of interest to note that while the σ_{inel} required to fit the emulsion average is considerably smaller than geometric, so that the nuclei are relatively transparent to K^+ mesons, the σ_{inel} for the three elements (for the same V and W) are in general not proportional to A; in fact they seem to depend also on V and T_K. This can be understood qualitatively as the effect partly of the bending of the trajectories of the incident particles in the long-range Coulomb field of the nucleus, and partly of the changed velocity of the K^+ meson inside the nucleus, although we have not studied these reasons too closely. In any case the procedure we have used is the correct one.

To show the effect of the emulsion average on the differential cross section we have plotted in Figs. 3 and 4 the separate contributions of Ag, Br, and N for typical cases of attractive and repulsive nuclear potentials. We observe first of all that everywhere in the repulsive case, and in the interference region in the attractive case, the contribution from N (approximating C, O, and N) is quite small, although not negligible. At larger angles in the attractive case, it is large enough to fill in the diffraction structure of the Ag and Br cross sections, but it is nowhere dominant. In any case both the large spread in q (or θ) and the large uncertainties of the experimental points in this region mean that the detailed shape of the curve is not important there. The approximation of replacing various light nuclei in the emulsion (principally C and O) by N is thus reliable and the use of the Fermi shape, with parameters appropriate to the heavier nuclei, in obtaining the N cross section is accurate enough in this angular region.

Secondly, we can remark on the actual shape of the cross sections in the region where the finite nuclear size is expected to produce diffraction structure. In the Born approximation the cases V and -V will show the same diffraction structure; the only difference will occur in the interference region, and for larger angles the Coulomb effects become unimportant. Even if the approximation is improved by including in the zero-order wave functions some of the distorting

effects of the Coulomb potential, this similarity between the V and the -V cross sections is expected to persist, because in the diffraction region they will still be proportional to V^2. We see that, in fact, this does not happen: whereas the -V cross sections show diffraction dips with the correct dependence on A, those for +V are almost smooth. This indicates that the scattering cannot be represented by such approximations. It also means that to the extent that the diffraction region is important in determining the nuclear potential, those analyses that have used the Born approximation or modification of it[1,4,8] are unreliable. In apparent disagreement with our results with repulsive potentials, the cross sections obtained by Cocconi et al,[3] using a partial-wave calculation, show considerable diffraction structure. These authors assumed a square-well potential, however, and it is well known that a finite skin-thickness has a pronounced effect on the cross section at large angles, making it both smoother and smaller. This means that the result of these authors as to the magnitude of V is not reliable. The same criticism can presumably be made of the phase-shift analysis of Costa and Patergnani,[2] used also later by Biswas et al,[5] and by Ceolin et al,[6] insofar as they try to predict the integrated elastic cross sections at large angles.

The next stage of the calculation, in which the differential cross sections are averaged over the energy range, is illustrated in Figs. 5 and 6. For lower energies, where the experimental data have been normalized so as to have the same effective track lengths at all energies, we take a simple, equally weighted average of cross sections at 45, 75 and 95 Mev. At the higher energy range, where the track-length distribution is as described in Fig. 1 we have averaged cross sections at 115, 150, and 185 Mev with respective weights 0.24:0.56:0.20, as previously discussed. The justification for using q, the recoil wave number, as independent variable is evident from these illustrations; while in other respects these cross sections are quite different from those predicted by the simple Born approximation, they are remarkably independent of energy when plotted against q. Thus the energy average does not wash out the detailed structure of the cross sections, which is the feature of principal interest in this problem. (It certainly does if cross sections are plotted against θ). For the lower-energy range this more than justifies the greater labor required to classify each scattering event according to q rather than just according to θ. Even for experiments that use a more-or-less monoenergetic beam of particles, such a property of the theoretical cross sections is of considerable use in comparing results at different energies.

The final results for the lower-energy range are presented in Figs. 7, 8, and 9. In obtaining the total cross section, we have used two values of θ_0. For $\theta_0 = 30^\circ$, the elastic cross section includes none of the interference region, and the object is only to obtain the magnitude of V. The total cross section for $\theta_0 = 8^\circ$, which was also calculated, includes the interference region. It is therefore, as information, not independent of the results shown in Fig. 8, where we have plotted the energy-averaged elastic differential cross section. The hope was to make better use of statistics on the question of the sign of the interference. The fact that for both $\theta_0 = 30^\circ$ and $\theta_0 = 8^\circ$ the same attractive as well as the same repulsive potentials gives agreement with experiment does, however, confirm our deduction of this fact from the plot of the differential cross sections. The results for some other values of V are shown in Fig. 9. They are in accord with the information given by Fig. 7, that only for sufficiently large values of V is the elastic differential cross section large enough at large angles to give agreement with experiment. We should explain that, because of the large amount of labor involved in investigating even one value of V, we have not made an exhaustive calculation of $\sigma_{total}(\theta > \theta_0)$ as a function of V, but have contented ourselves with making calculations only at the indicated points, sketching in the remaining curve. We do not think that this affects the conclusions appreciably. These results differ from those reached by several authors[1-8] who analyzed data in the same energy interval. They concluded that the data could not be fitted with an attractive potential.

In view of the results in the higher-energy range, which we shall describe presently, it is perhaps only of academic interest that the conclusions we have just come to differ from those of previous authors on the very important question of the sign of V. It seems to us that in the work of previous authors, even where a partial wave calculation was made, there was no real attempt to fit the data with an attractive nuclear potential. We would say that it is very difficult to detect the sign of V at the low energies, because of the fact that in the interference region the structure has been so washed out by the imaginary part of the potential and by the averaging over the emulsion.

Fortunately, the situation at the higher energies is unambiguous. We see from Fig. 10 that there is both a positive and a negative value of V for which $\sigma_{total}(\theta < 10^\circ)$ is in agreement with experiment. Of the differential cross

sections for these two cases, however, only that for the positive V is in good agreement with experiment. Our ability to throw out the curve for negative V is due partly to the improved statistics of the experiments at the higher energy, but mainly to the fact that the structure of the theoretical curves is less washed out by the imaginary potential and by the averaging procedures. From the other theoretical cross sections in Fig. 11, this is seen to be true in general for attractive potentials.

If we believe that the sign of the potential does not change in going from about 75 Mev to 150 Mev, we must then conclude that the nuclear potentials are as follows:

$$T_K = 40 \text{ to } 100 \text{ Mev}: \quad V = 27 \pm 8 \text{ Mev}, \quad W = -5.7 \pm 1.1 \text{ Mev};$$

$$T_K = 150 \pm 30 \text{ Mev}: \quad V = 27 \pm 3 \text{ Mev}, \quad W = -10.3 \pm 1.6 \text{ Mev}.$$

It is rather difficult to be sure of the errors on these quantities; those shown for V are due to statistics in $\sigma_{total}(\theta > 30^o)$ and $\sigma'_{total}(\theta > 10^o)$ in the two cases respectively; and those for W are due to statistics in σ_{inel}.

CONCLUSIONS

The imaginary potential W can be related by simple semiclassical arguments to the average K^+-nucleon cross section ($\bar{\sigma}$) inside the nucleus; the result is that

$$\bar{\sigma} = 2W (\hbar v \rho_0 \eta)^{-1} , \tag{7}$$

where v and ρ_0 are the velocity of the K^+ mesons and the nucleon density, both taken <u>inside</u> the nucleus and η is a correction factor that allows for the effect of the Pauli principle on the collisions inside the nucleus, and has been calculated by Sternheimer.[13] For a matter distribution of the Fermi shape, ρ_0 is given

$$\rho_0 = A \left[(4\pi r_0^3/3)(1 + 9.88\, d^2/r_0^2) \right]^{-1} . \tag{8}$$

Substitution of our values of V and W then leads to

$$T_K = 40 \text{ to } 100 \text{ Mev}, \ \bar{\sigma} = 21 \pm 8 \text{ mb};$$

$$T_K = 150 \pm 30 \text{ Mev}, \ \bar{\sigma} = 13 \pm 2 \text{ mb}.$$

The rather large quoted errors on the result for the low-energy range come both directly from the uncertainty in W, and indirectly through the influence on η and v of the uncertainty in V. It is also possible that Sternheimer's calculation of η as a universal factor may not be reliable for the low energies, where it has a 50% effect on $\bar{\sigma}$. The result is in good agreement with the values quoted as $\bar{\sigma}_5$ in Table II in Ref. 9. The resulting K^+-hydrogen and K^+-neutron cross section have been discussed in Ref. 9.

The result for the high-energy range is probably not too dependent on our initial choice of radial parameters for the potential, although with a larger radius we should have needed a smaller W to fit σ_{inel}, the nucleon density ρ_0 would be correspondingly smaller, and the influence of the value of V on v and η is unimportant. At the low energies the last statement is no longer true, but the only way to find out the dependence of V and W on the assumed nuclear size is to repeat the whole calculation with a different radius, and this we have not found the energy to do. It is certainly not clear that the choice is unimportant or easily corrected for, but we feel that the choice we made is the most reasonable on the basis of our present knowledge of nuclei.

These last remarks introduce a justification of some assumptions we have not as yet commented on: we have assumed that V and W are independent of A and T_K in each energy range. A theoretical deviation of V and W from some assumed K^+-nucleon interaction would presumably give them to be proportional to ρ_0 at least for nuclei as large as Ag or Br. Our formula, with our assumption about r_0 and d, gives for ρ_0 values for Ag and Br that differ by only 2%. Because the contribution from N has been seen to be not very important, it does not matter that our assumptions

about the shape of this nucleus and about the constancy of V and W are not very good. As regards the variation with T_K, our results show that as T_K doubles ($T_K \sim 75$ Mev to 150 Mev) W almost doubles. It is thus in principle necessary to redo the whole calculation, building in this first approximation to the energy dependence of W. We do not believe that this would alter our conclusions appreciably, and certainly not in the high-energy range.

To summarize the calculations, we have found from an examination of experiments in the two energy ranges $T_K = 40$ to 100 Mev and $T_K = 150 \pm 30$ Mev that the nuclear potential for K^+ mesons is repulsive, and about 27 Mev at both energies. The imaginary potential, after allowance for the Pauli principle, is at both energies compatible with a K-nucleon cross section of the same size as that measured for free protons.

ACKNOWLEDGMENTS

We wish to thank the authorities of the Los Alamos Scientific Laboratory for the use of the IBM 704 Computer on which the phase shift calculations were performed, and particularly Dr. David L. Hill for making the necessary arrangements for the use of these computer facilities. We are grateful to Mrs. Frances Glenn, Miss Graydon Hindley, Miss Helen Probst, Miss Harriett Rice, and Mrs. Catherine Toche for their careful scanning and measurements and assistance in compiling the data.

This work was supported in part by the U.S. Air Force through the Air Force Office of Scientific Research, Air Research and Development Command, and in part by the U.S. Atomic Energy Commission.

REFERENCES

*Now at the University of Illinois, Urbana, Illinois

**Now at General Electric Research Laboratories, Schenectady, New York

†Now at Florida State University, Tallahassee, Florida

††Present address: Massachusetts Institute of Technology, Cambridge, Massachusetts.

1. L.S. Osborne, Phys. Rev. 102, 296 (1956).
2. G. Costa and G. Patergnani, Nuovo Cimento 5, 448 (1957).
3. Cocconi, Puppi, Quareni, and Stanghellini, Nuovo Cimento 5, 172 (1957).
4. Hoang, Kaplon, and Cester (to be published).
5. Biswas, Ceccarelli-Fabbrichesi, Ceccarelli-Gottstein, Varshneya, and Waloschek, Nuovo Cimento 5, 123 (1957).
6. Ceolin, Cresti, Dallaporta, Grilli, Guerriero, Merlin, Salandin, and Zago, Nuovo Cimento 5, 402 (1957).
7. Bhowmik, Evans, Nilsson, Prowse, Anderson, Keefe, Kerman, and Losty (to be published).
8. D. Fournet-Davis, Phys. Rev. 106, 816 (1957).
9. Lannutti, Goldhaber, Goldhaber, Chupp, Giambuzzi, Marchi, Quareni, and Watghin (to be published).
10. We ignore relativistic effects, except in the kinematics of the scattering. For the higher energies, v^2/c^2 is about 0.5.
11. Hahn, Ravenhall, and Hofstadter, Phys. Rev. 101, 1131 (1956).
12. Because the criterion for inelasticity is that $\Delta T/T \geq 10\%$, what we assume to be elastic scattering could possibly include inelastic scattering that involves excitation of low-lying nuclear levels. It is difficult to examine the effect theoretically, but estimates we have made, using electron-scattering results as a guide, indicate that in the interference region it is negligible, while at large angles, where we deal only with the total cross section (elastic plus inelastic), it is immaterial.
13. R.M. Sternheimer, Phys. Rev. 106, 1027 (1957).
14. The $K^{\pm}$ hydrogen cross section measured in a propane bubble chamber (Meyer, Perl, and Glaser, Phys. Rev. 107, 279 (1957) of 9.4 ± 1.7 mb, for T_K = 20 to 90 Mev, is somewhat lower than the emulsion result in the energy region. The reason for the difference is not clear, but it is probable that the difference is not statistically significant.

FIGURE CAPTIONS

1. Path length distribution observed. The dashed distribution is the resulting approximation obtained by using the weighting factors given.
2. Differential cross section for the scattering of 75-Mev K^+ mesons from silver, with a real potential of -20 Mev. The two curves are for W = 0 (no absorption) and for W = - 4.1 Mev, which gives the observed σ_{inel}. They show the marked effect of including W on the shape of the elastic cross section. This, and the following figures up to Fig. 9, are for the energy range T_K = 40 to 100 Mev.
3. Differential cross sections at 75 Mev for silver, bromine, and nitrogen, for the attractive potential V = - 45 Mev, W = - 3.8 Mev, to illustrate the contributions of the elements of the emulsion.
4. The corresponding situation to that of Fig. 3, for the repulsive potential V = 25 Mev, W = - 5.6 Mev.
5. Differential cross sections for the emulsion, at 45, 75, and 95 Mev, for the attractive potential V = - 45 Mev, W = - 3.8 Mev. They illustrate the contributions of the various parts of the energy range.
6. The corresponding situation to that of Fig. 5, for the repulsive potential V = 25 Mev, W = - 5.6 Mev.
7. The total cross section (elastic plus inelastic) for angles greater than θ_0, plotted against V, for $\theta_0 = 8^\circ$ and $\theta_0 = 30^\circ$. It has been averaged over the elements of the emulsion and over the energy range T_K = 40 to 100 Mev. The horizontal lines mark the experimental values[9] with standard deviations. The calculations were made only for the indicated points, and the curve was sketched in.
8. Differential cross sections averaged over the emulsion and over energy for the two potentials whose total cross sections agree with experiment. They are V = 25 Mev, W = - 5.6 Mev and V = - 45 Mev, W = - 3.8 Mev.
9. Differential cross sections averaged over the emulsion and over energy for the two potentials of the previous figure, and also for V = 10 Mev, W = - 4.9 Mev and V = - 20 Mev, W = - 4.1 Mev to show the effect of varying V.
10. The corresponding situation to that of Fig. 7 for T_K = 150 ± 30 Mev, and $\theta_0 = 10^\circ$.

11. The corresponding situation to that of Fig. 8 for the energy range $T_K = 150 \pm 30$ Mev and for the potentials V = 35 Mev, W = - 10.7 Mev; V = 25 Mev, W = - 10.6 Mev, V = - 15 Mev, W = - 9.1 Mev; V = - 30 Mev, W = - 8.8 Mev; and V = - 40 Mev, W = - 8.2 Mev. The results at larger angles are shown in the inset figure.

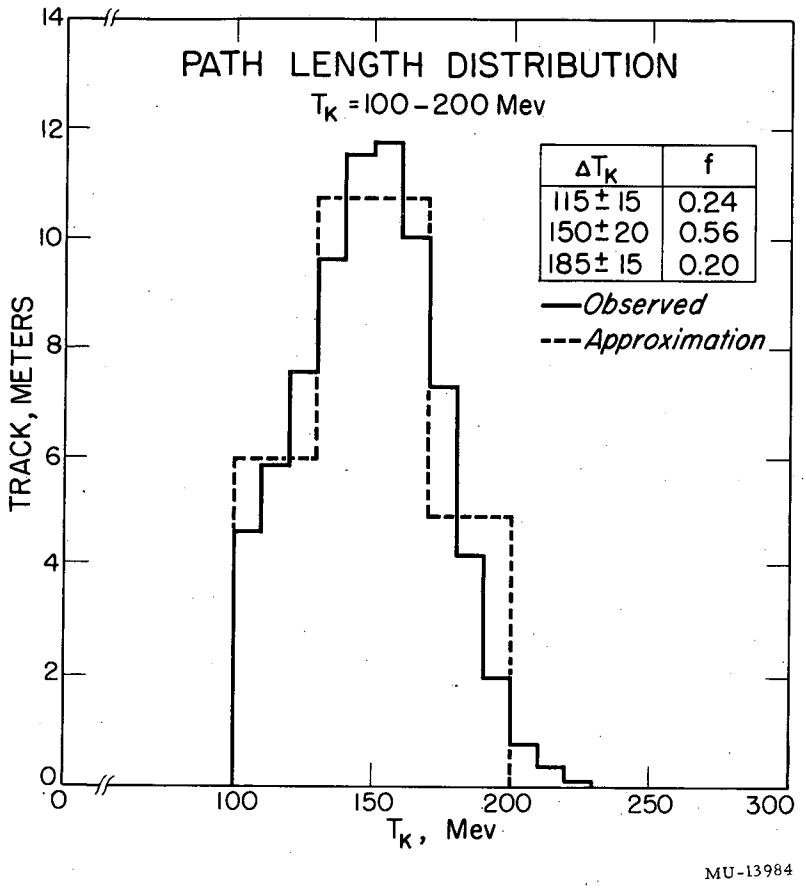
PATH LENGTH DISTRIBUTION
T_K = 100 – 200 Mev
ΔT_K | f
115 ± 15 | 0.24
150 ± 20 | 0.56
185 ± 15 | 0.20
—Observed
---Approximation
TRACK, METERS
T_K, Mev
0
2
4
6
8
10
12
14
100
150
200
250
300
MU-13984

Fig. 1

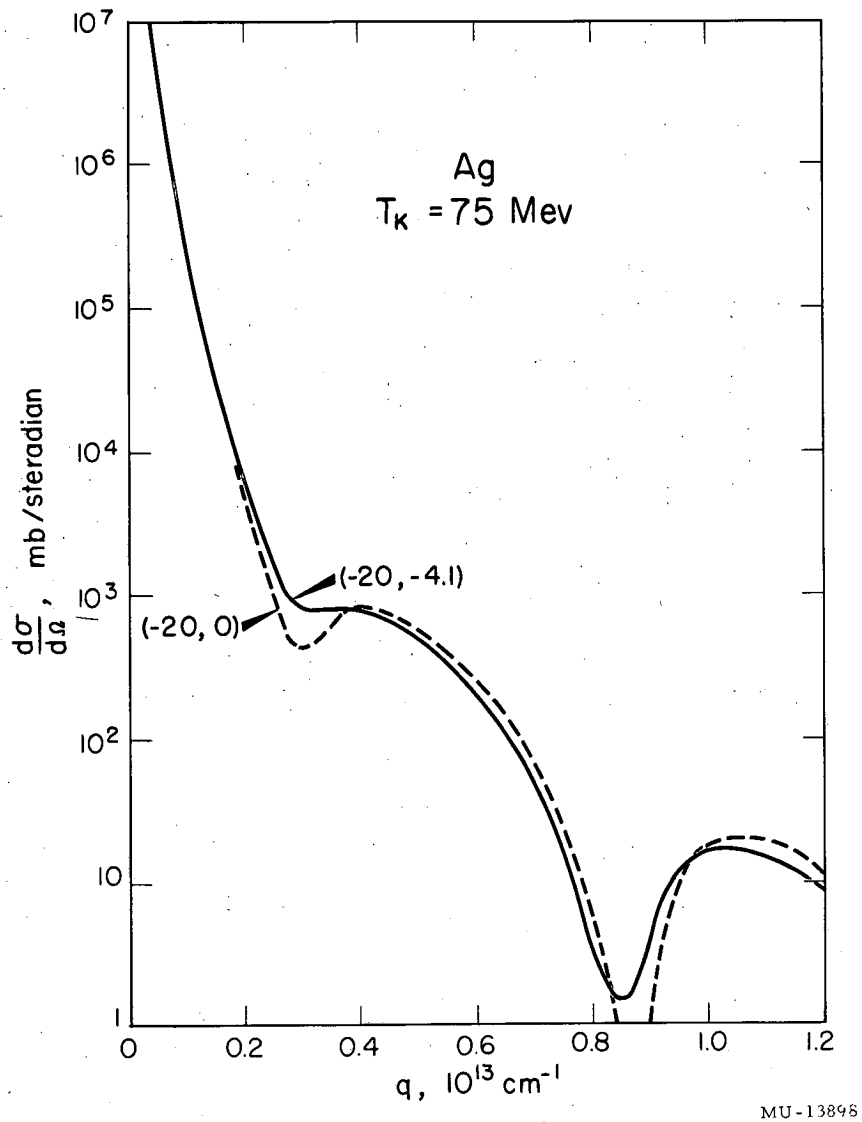
Ag
T_K = 75 Mev
(-20, -4.1)
(-20, 0)
$\frac{d\sigma}{d\Omega}$, mb/steradian
10^7
10^6
10^5
10^4
10^3
10^2
10
1
0
0.2
0.4
0.6
0.8
1.0
1.2
q, 10^{13} cm^{-1}
MU-13898

Fig. 2

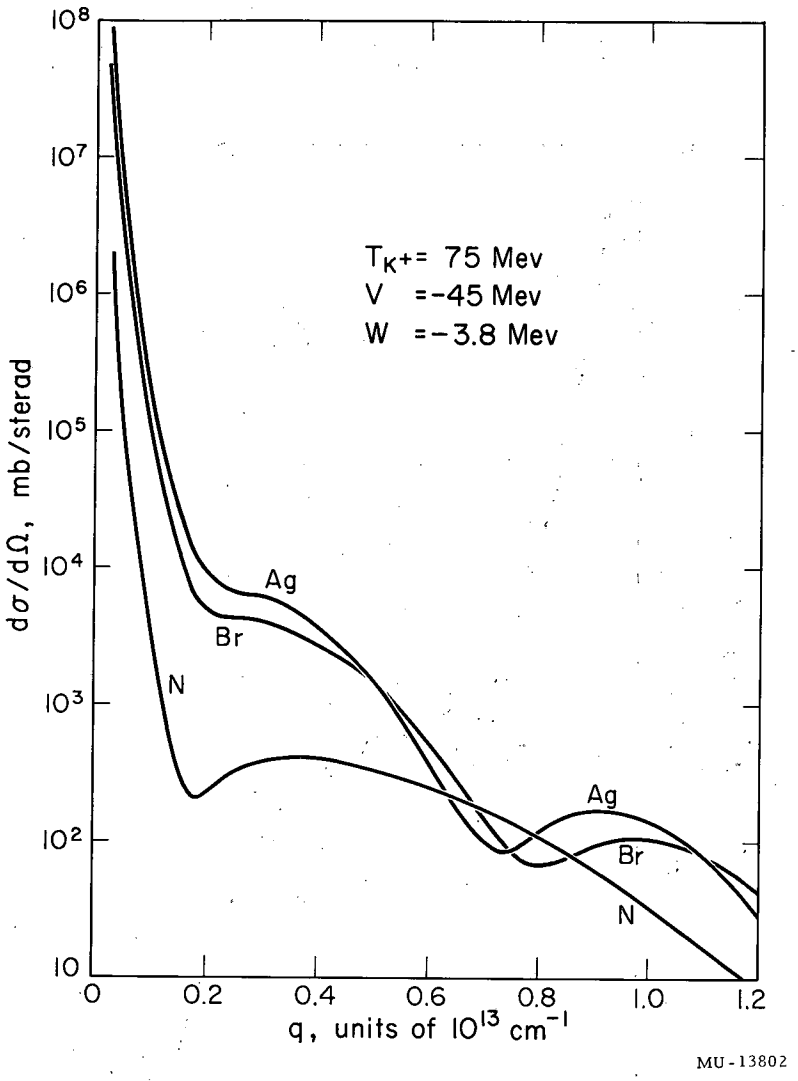
10^8
10^7
10^6
10^5
10^4
10^3
10^2
10
$d\sigma/d\Omega$, mb/sterad
T_{K^+}= 75 Mev
V =-45 Mev
W =-3.8 Mev
Ag
Br
N
Ag
Br
N
0
0.2
0.4
0.6
0.8
1.0
1.2
q, units of 10^{13} cm^{-1}
MU-13802

Fig. 3

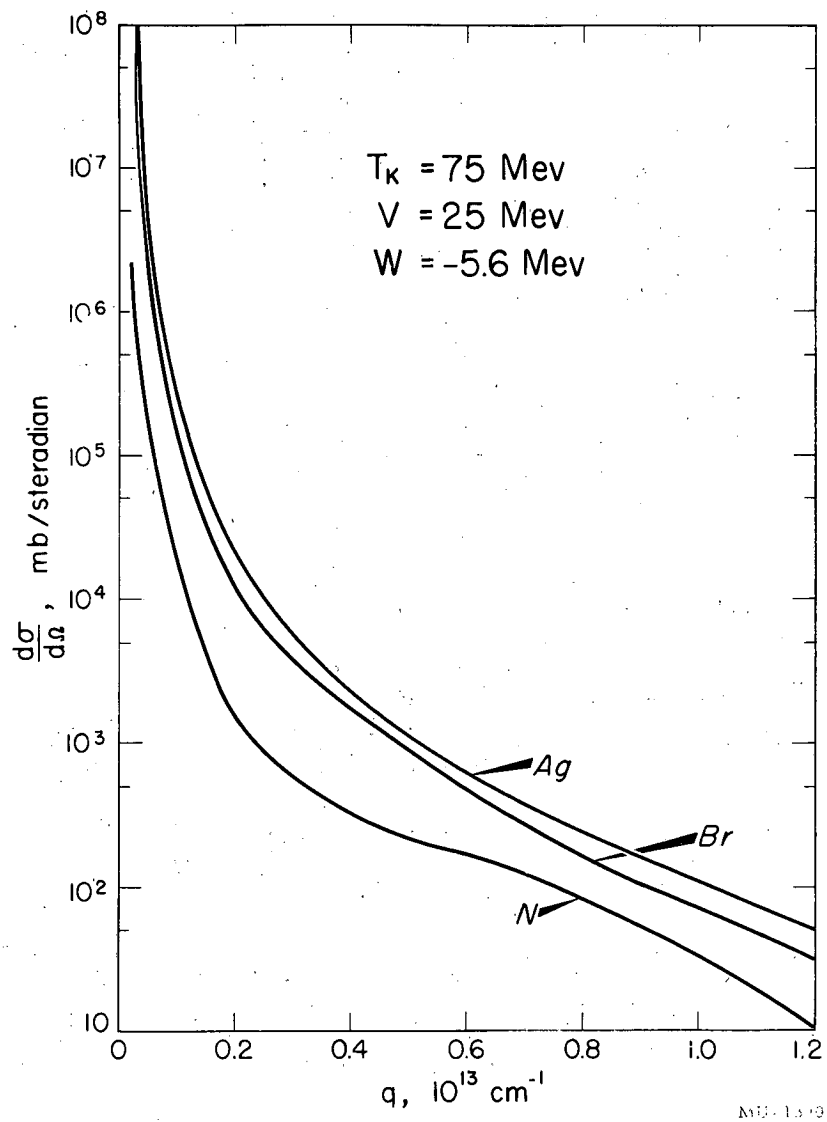
T_K = 75 Mev
V = 25 Mev
W = -5.6 Mev
Ag
Br
N
$\frac{d\sigma}{d\Omega}$, mb/steradian
q, 10^{13} cm^{-1}
10^8
10^7
10^6
10^5
10^4
10^3
10^2
10
0
0.2
0.4
0.6
0.8
1.0
1.2

Fig. 4

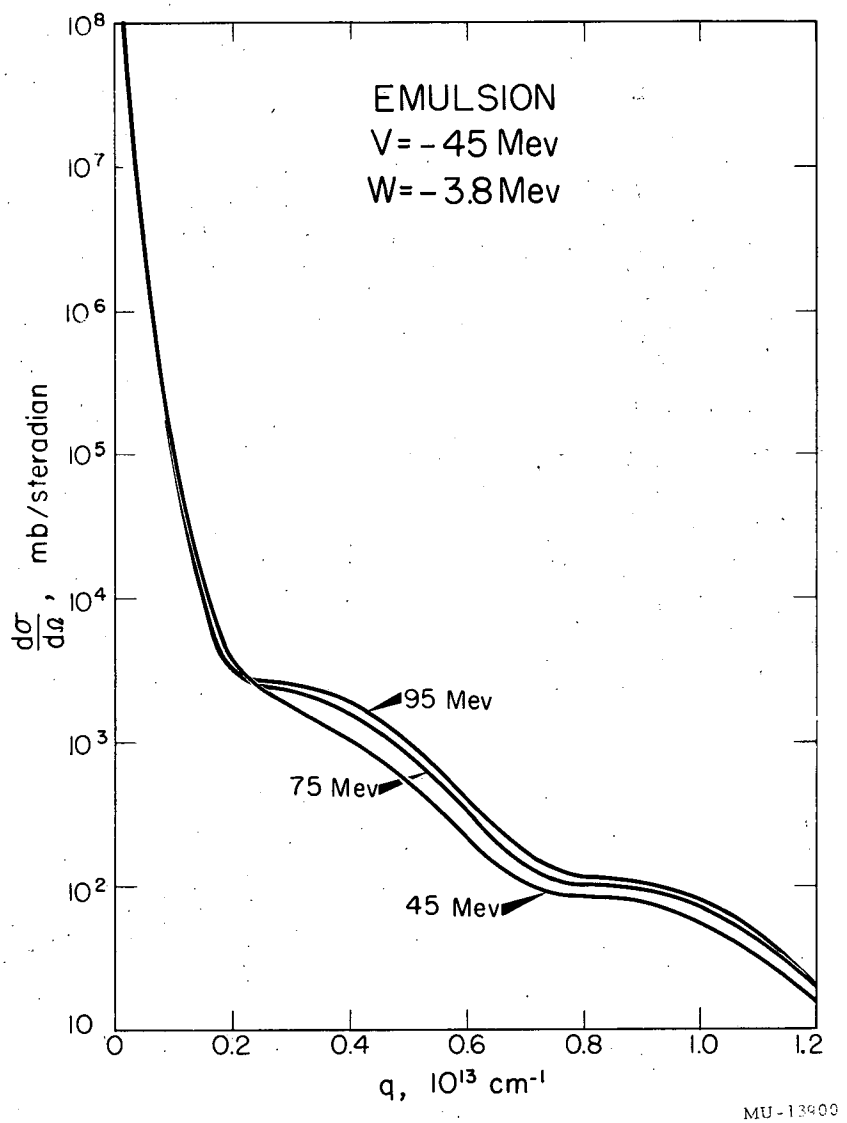
EMULSION
V = -45 Mev
W = -3.8 Mev
95 Mev
75 Mev
45 Mev
$\frac{d\sigma}{d\Omega}$, mb/steradian
q, 10^{13} cm^{-1}
10^8
10^7
10^6
10^5
10^4
10^3
10^2
10
0
0.2
0.4
0.6
0.8
1.0
1.2
MU-13900

Fig. 5

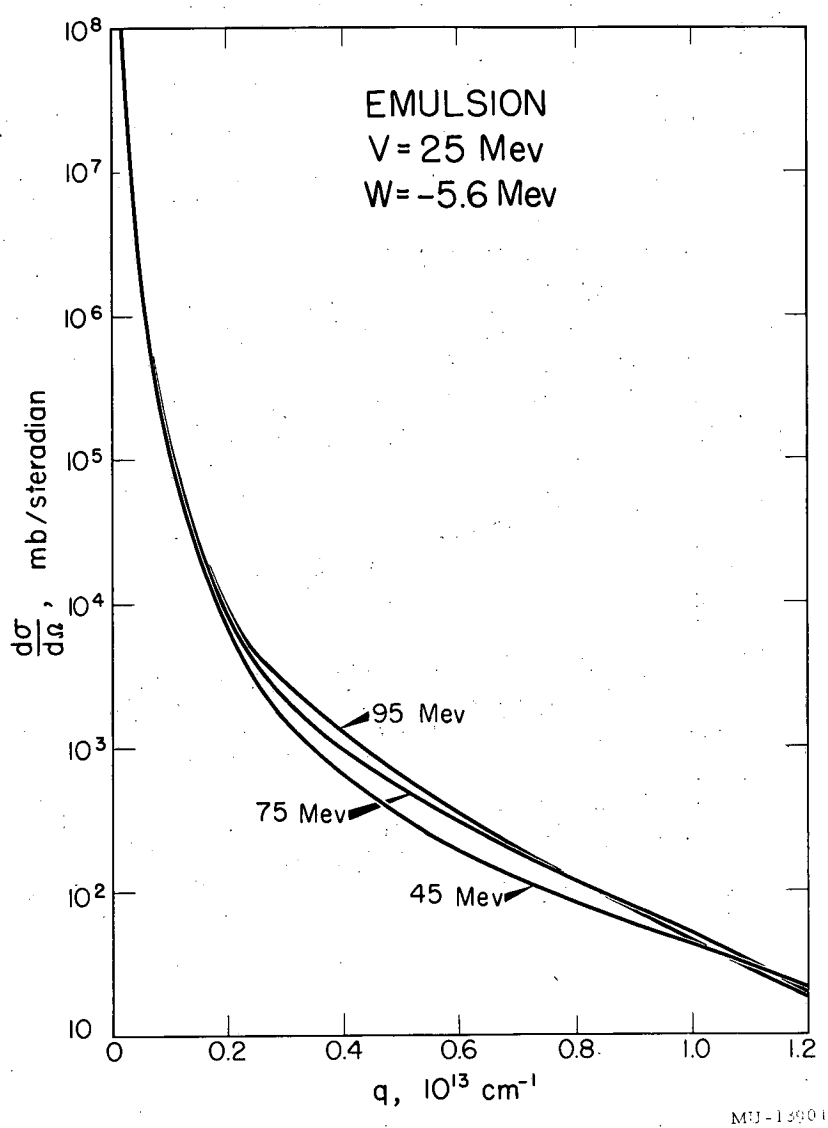
EMULSION
V = 25 Mev
W = -5.6 Mev
95 Mev
75 Mev
45 Mev
$\frac{d\sigma}{d\Omega}$, mb/steradian
q, 10^{13} cm^{-1}
10^8
10^7
10^6
10^5
10^4
10^3
10^2
10
0
0.2
0.4
0.6
0.8
1.0
1.2
MU-13901

Fig. 6

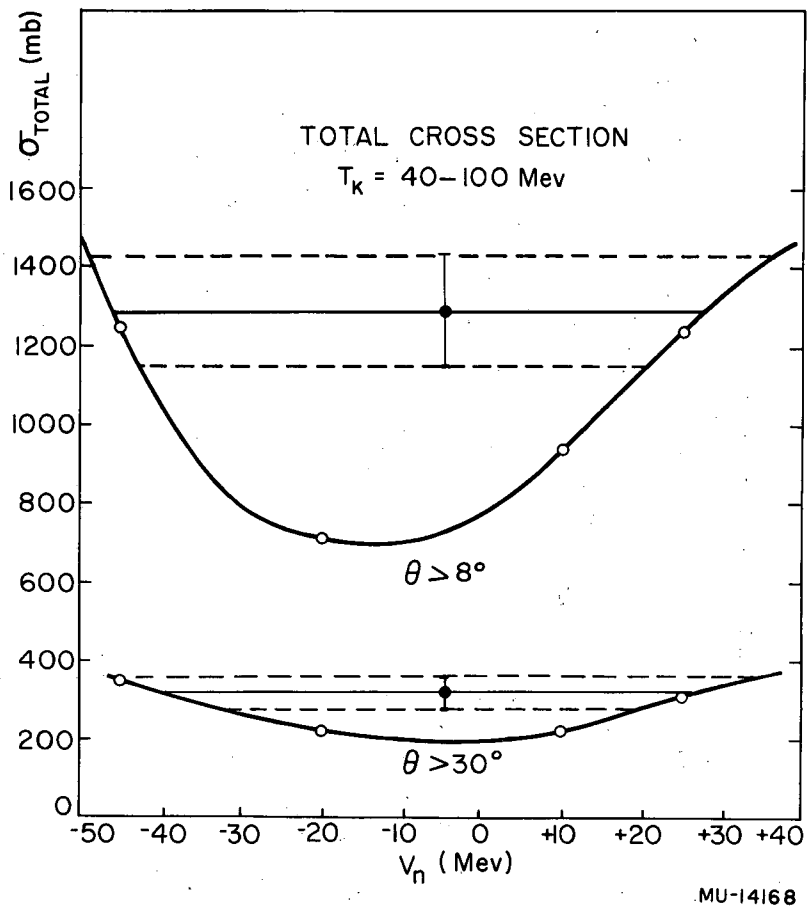
σ_{TOTAL} (mb)
TOTAL CROSS SECTION
T_K = 40–100 Mev
1600
1400
1200
1000
800
600
400
200
0
$\theta > 8°$
$\theta > 30°$
-50 -40 -30 -20 -10 0 +10 +20 +30 +40
V_n (Mev)
MU-14168

Fig. 7

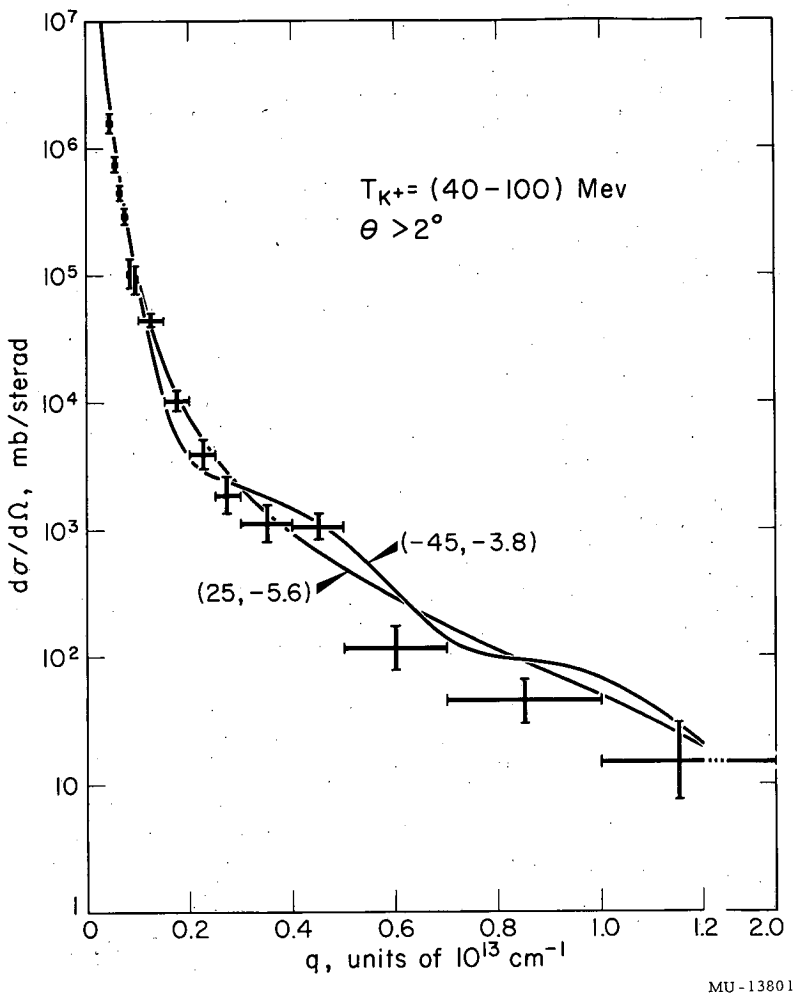
T_{K^+}= (40-100) Mev
θ >2°
(-45, -3.8)
(25, -5.6)
$d\sigma/d\Omega$, mb/sterad
q, units of 10^{13} cm^{-1}
10^7
10^6
10^5
10^4
10^3
10^2
10
1
0
0.2
0.4
0.6
0.8
1.0
1.2
2.0
MU-13801

Fig. 8

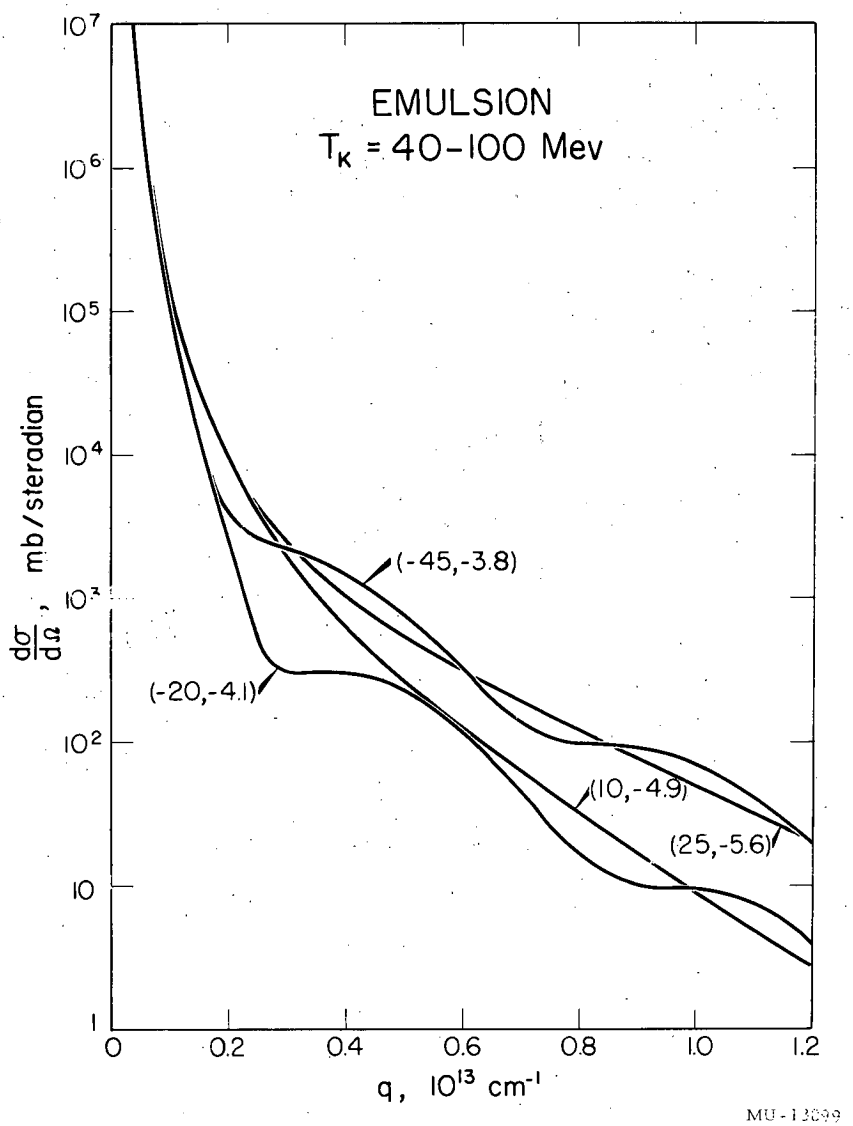
EMULSION
T_K = 40-100 Mev
10^7
10^6
10^5
10^4
10^3
10^2
10
1
$\frac{d\sigma}{d\Omega}$, mb/steradian
(-45,-3.8)
(-20,-4.1)
(10,-4.9)
(25,-5.6)
0
0.2
0.4
0.6
0.8
1.0
1.2
q, 10^{13} cm^{-1}
MU-13699

Fig. 9

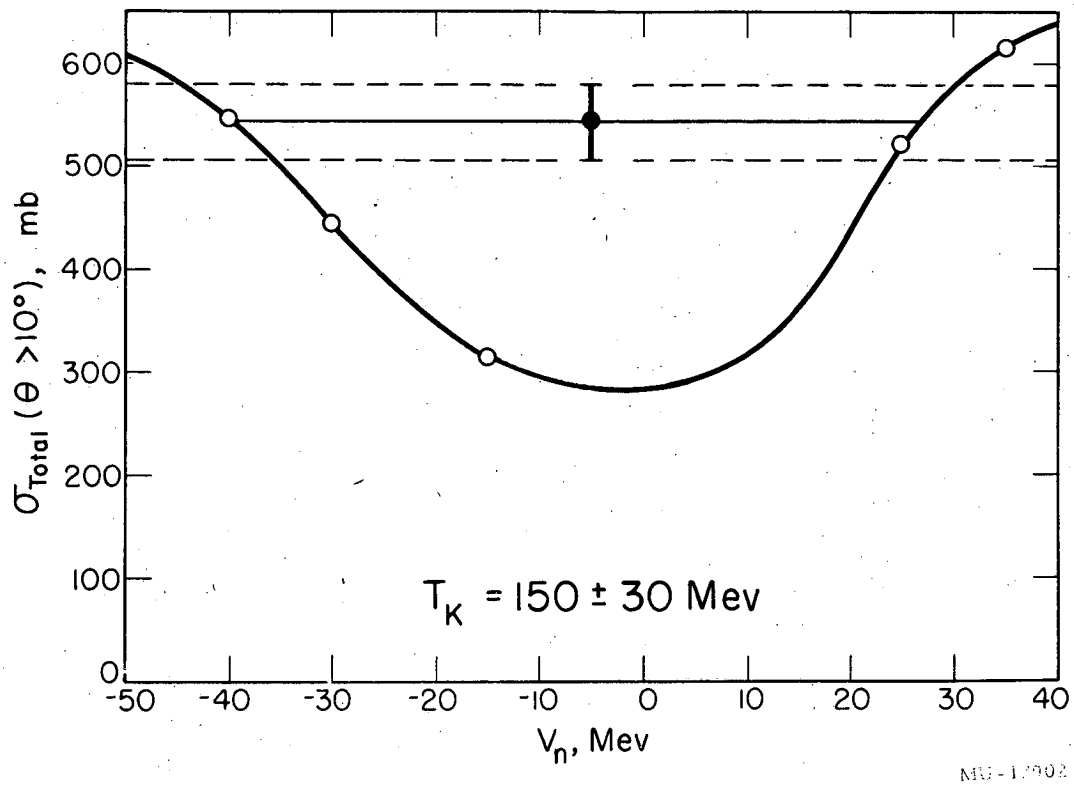
600
500
400
300
200
100
0
σ_{Total} (θ >10°), mb
T_K = 150 ± 30 Mev
-50
-40
-30
-20
-10
0
10
20
30
40
V_n, Mev

Fig. 10

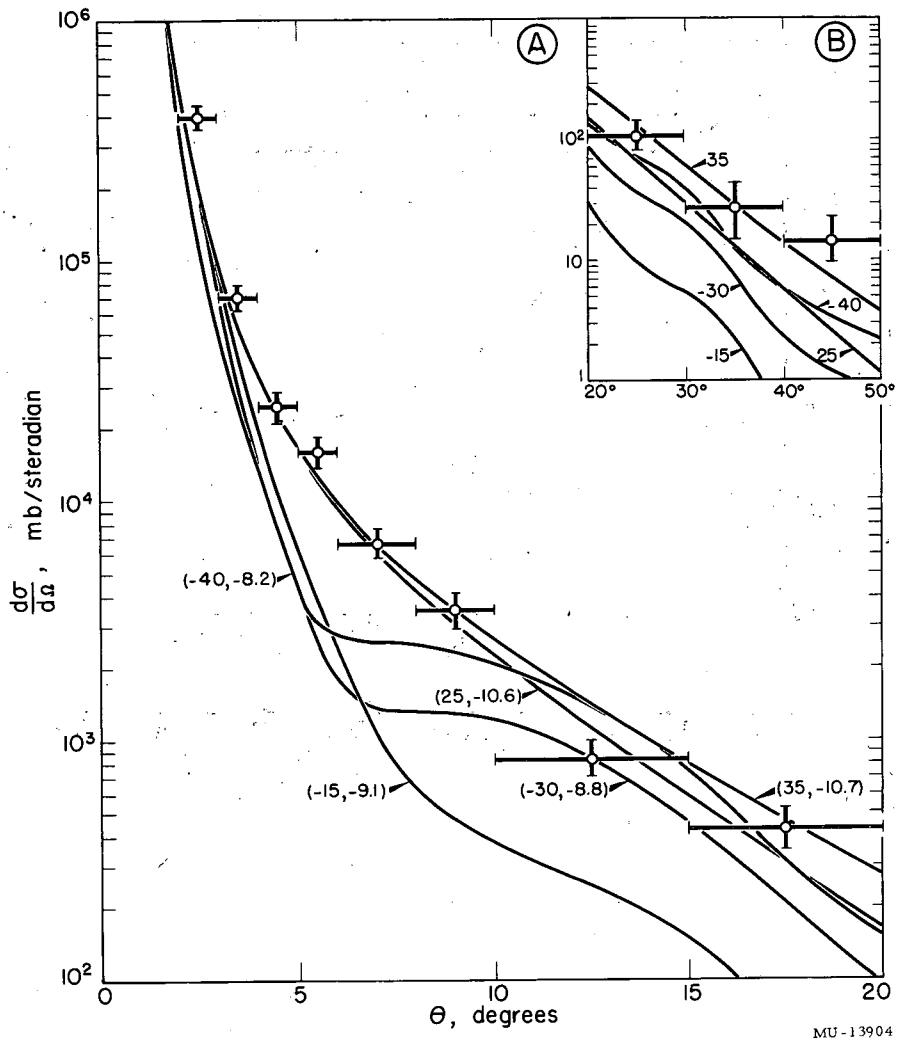
A
B
10^6
10^5
10^4
10^3
10^2
$\frac{d\sigma}{d\Omega}$, mb/steradian
0
5
10
15
20
θ, degrees
(-40,-8.2)
(25,-10.6)
(-15,-9.1)
(-30,-8.8)
(35,-10.7)
35
-30
-40
-15
25
1
20°
30°
40°
50°
MU-13904

Fig. 11